Electrical Conduction Behavior of Cement-Matrix Composites

D.D.L. Chung

(Submitted 26 March 2000; in revised form 9 October 2001)

In this work, the electrical conduction behavior of cement-matrix composites is reviewed, with a focus on the resistive, thermoelectric and electromagnetic behavior, in addition to the effect of strain and of damage on the resistive behavior. Admixtures such as short fibers are effective for enhancing the electrical behavior and for providing p-type and n-type cement matrix composites.

Keywords cement, composite, concrete, electromagnetic, thermoelectric, piezoresistive, resistive

1. Introduction

As structural materials, cement-matrix composites have received much attention in terms of their mechanical properties, but relatively little attention in terms of their electrical conduction properties. Nevertheless, the electrical properties are relevant to the use of the structural materials for non-structural purposes such as sensing and electromagnetic interference (EMI) shielding. The ability to provide non-structural functions allows a structural material to be multifunctional, thus saving cost and enhancing durability. Furthermore, the electrical properties shed light on the structure of the materials, particularly concerning the interfaces in the composite materials. Therefore, for both technological and fundamental reasons, the electrical properties of cement-matrix composites are of interest and constitute the subject of this review. This review addresses the resistive, piezoresistive, thermoelectric, and electromagnetic behavior of cement-matrix composites.

2. Resistive Behavior

Cement paste is electrically conductive, with DC resistivity at 28 days of curing around 5×10^3 Ω.m at room temperature. The resistivity is increased slightly (to 6×10^3 Ω.m), by the addition of silica fume (SiO_2 particles around 0.1 μm in size, in the amount of 15% by weight of cement), and increased more (to 7×10^3 Ω.m) by addition of latex (20% by weight of cement), which is a styrene-butadiene copolymer in the form of particles of size around 0.2 μm.[1,2] The higher the latex content, the higher the resistivity is.[3] In case of mortars (with fine aggregate, i.e., sand), the transition zone between the cement paste and the aggregate enhances the conductivity.[4] Whether aggregates (sand and stones) are present or not, the AC impedance spectroscopy technique for characterizing the frequency-dependent electrical behavior is useful for studying the microstructure.[4-14]

D.D.L. Chung, Composite Materials Research Laboratory, State University of New York at Buffalo, Buffalo, NY 14260-4400. Contact e-mail: ddlchung@acsu.buffalo.edu.

The admixture effects mentioned above are small compared to the effect of adding short (5 mm) carbon fibers (0.5% by weight of cement), which decrease the resistivity to 2×10^2 Ω.m in the presence of silica fume and to 1×10^3 Ω.m in the presence of latex.[1,2] The lower resistivity when silica fume is present along with the carbon fibers than when latex is present is due to the greater degree of fiber dispersion provided by silica fume than by latex.[15] The fiber content mentioned above corresponds to 0.48 vol.% in the presence of silica fume and to 0.41 vol.% in the presence of latex. These volume fractions are below the percolation threshold.[16,17] (Percolation refers to the situation in which there is a continuous electrical conduction path formed by the fibers due to the contact between adjacent fibers in the composite.) Increasing the fiber content to 1.0% by weight of cement decreases the resistivity much more—to 8 Ω.m in the presence of silica fume and to 20 Ω.m in the presence of latex.[1,2]

Figure 1[16] shows the volume electrical resistivity of carbon-fiber composites at 7 days of curing.[16] The resistivity decreases greatly with increasing fiber volume fraction whether a second filler (silica fume or sand) is present or not. When sand is absent, the addition of silica fume decreases the resistivity at all carbon fiber volume fractions except the highest volume fraction of 4.24%; the decrease is most significant at the lowest fiber volume fraction of 0.53%. When sand is present, the addition of silica fume similarly decreases the resistivity, such that the decrease is most significant at fiber volume fractions below 1%. When silica fume is absent, the addition of sand decreases the resistivity only when the fiber volume fraction is below about 0.5%; at high fiber volume fractions, the addition of sand even increases the resistivity due to the porosity induced by the sand. Thus the addition of a second filler (silica fume or sand) that is essentially non-conducting decreases the resistivity of the composite only at low volume fractions of the carbon fibers, and the maximum fiber volume fraction for the resistivity to decrease is larger when the particle size of the filler is smaller. The resistivity decrease is attributed to the improved fiber dispersion due to the presence of the second filler. Consistent with the improved fiber dispersion is the increased flexural toughness and strength due to the presence of the second filler.[15]

The use of both silica fume and sand results in an electrical resistivity of 3.19×10^3 Ω.cm at a carbon fiber volume fraction of just 0.24 vol.%. This is an outstandingly low resistivity value compared to those of polymer-matrix compos-

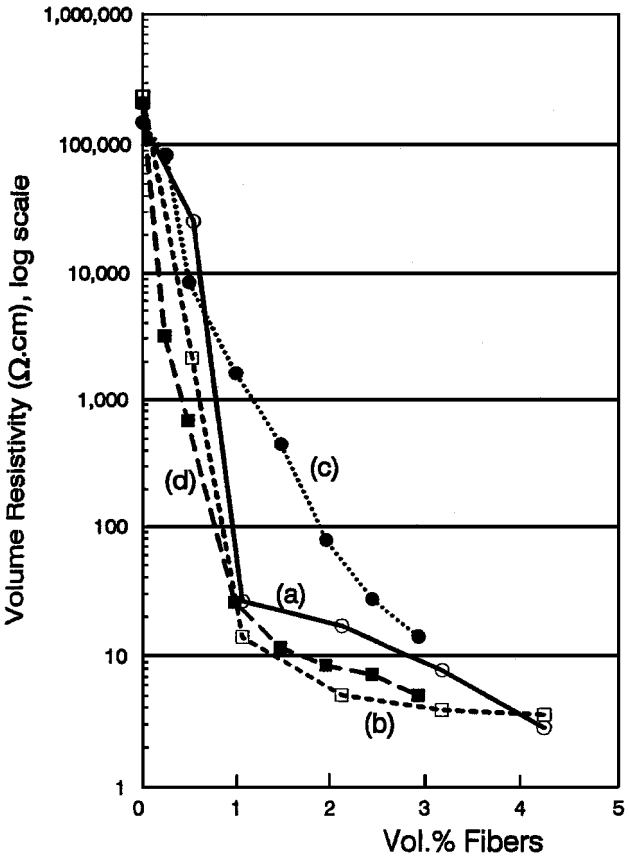

Fig. 1 Variation of the volume electrical resistivity with carbon fiber volume fraction. **(a)** Without sand, with methylcellulose, without silica fume; **(b)** without sand, with methylcellulose, with silica fume; **(c)** with sand, with methyscellulose, without silica fume; **(d)** with sand, with methyscellulose, with silica fume

ites with discontinuous conducting fillers at similar volume fractions.

Electrical conduction in cement reinforced by short carbon fibers below the percolation threshold is governed by carrier hopping across the fiber-matrix interface. The activation energy is decreased by increasing the fiber crystallinity, but is increased by using intercalated fibers. The carbon fibers contribute to hole conduction, which is further enhanced by intercalation, thereby decreasing the absolute thermoelectric power and the resistivity.[18]

Electric polarization induces an increase of the measured electrical resistivity of carbon fiber reinforced cement paste during resistivity measurement.[19] The effect is diminished by increasing the conductivity of the cement paste through the use of carbon fibers that are more crystalline, the increase of the fiber content, or the use of silica fume instead of latex as an admixture. Intercalation of crystalline fibers further increases the conductivity of the composite, but it increases the extent of polarization.[18] Voltage polarity switching effects are dominated by the polarization of the sample itself when the four-probe method is used, but are dominated by the polarization at the contact-sample interface when the two-probe method is used. Polarization reversal is faster and more complete for the latter.[19]

The curing age has relatively minor influence on the electrical resistivity, although it has major influence on the mechanical properties. From a curing age of 1 day to 28 days, the resistivity is increased by 63% for plain mortar, by 18% for latex mortar, by 18% for carbon fiber (0.53 vol.%) latex mortar, and by 4% for carbon fiber (1.1 vol.%) latex mortar.[20] Because the resistivity is a quantity that can vary by orders of magnitude, the percentage increases mentioned above do not reflect a large effect. Nevertheless, the effect in the absence of conducting fibers, especially in terms of the impedance, is sufficient for use in studying the curing process.[21-43] An increase in the carbon fiber content from 0.53 to 1.1 vol.% diminishes the effect of curing age significantly because the fibers become more dominant in governing the resistivity as the fiber content increases. The addition of latex also diminishes the effect of curing age.

Short steel fibers used as an admixture in cement paste also decrease the resistivity, such that the resistivity is lower in the presence of silica fume than in the presence of latex.[44] The contact electrical resistivity between stainless steel fiber and cement paste is around 6×10^2 $\Omega.m^2$ and is smaller if the fiber has been acid washed.[45]

Fundamentally, the main difference between carbon fibers and steel fibers is that carbon fibers contribute to hole conduction whereas steel fibers contribute to electron conduction,[2,44] as indicated by thermoelectric power measurement. Another difference is that the contact resistivity decreases with increasing bond strength for carbon fibers, due to the effect of interfacials voids, whereas the contact resistivity increases with increasing bond strength for steel fibers, due to the effect of the interfacial oxide phase.[45,46]

The interface between steel fiber and cement matrix behaves similarly to that between steel reinforcing bar (rebar) and concrete. The latter is more common in practice than the former. The contact resistivity of the latter interface is around 6×10^3 $\Omega.m^2$.[47]

The insulating behavior of cement-matrix composites is relevant to the use as substrates for electronic packaging and as high voltage insulation. The attainment of a high resistivity requires thorough drying, as moisture decreases the resistivity.[48,49] Chloride and sulphate contamination also decrease the resistivity.[50] A resistivity as high as 10^{10} $\Omega.m$ has been attained.[48-52]

3. Effect of Temperature on Resistive Behavior

The dependence of the resistivity on temperature provides information on the energetics and mechanism of electrical conduction. Furthermore, this dependence allows the cement-matrix composite to serve as a thermistor, which is a thermometric device consisting of a material (typically a semiconductor, but in this case a cement-matrix composite) whose electrical resistivity decreases with a rise in temperature.

Figure 2[1] shows the current-voltage characteristic of carbon fiber (0.5% by weight of cement) silica fume (15% by weight of cement) cement paste at 38 °C during stepped heating. The characteristic is linear below 5 V and deviates positively from linearity beyond 5 V. The deviation from linearity is due to Joule heating. The resistivity is obtained from the slope of the linear portion. The voltage at which the charac-

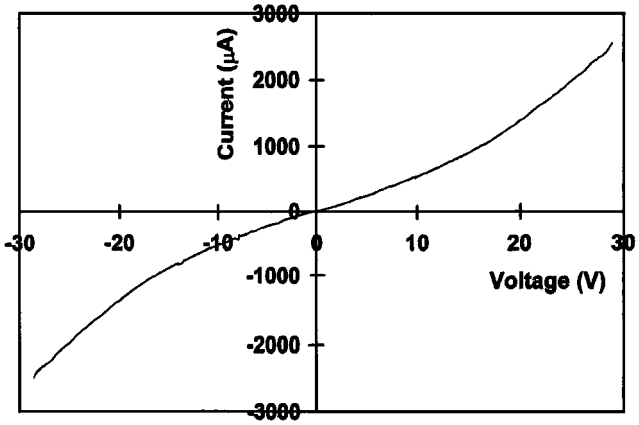

Fig. 2 Current-voltage characteristic of carbon-fiber silica-fume cement paste at 38 °C during stepped heating

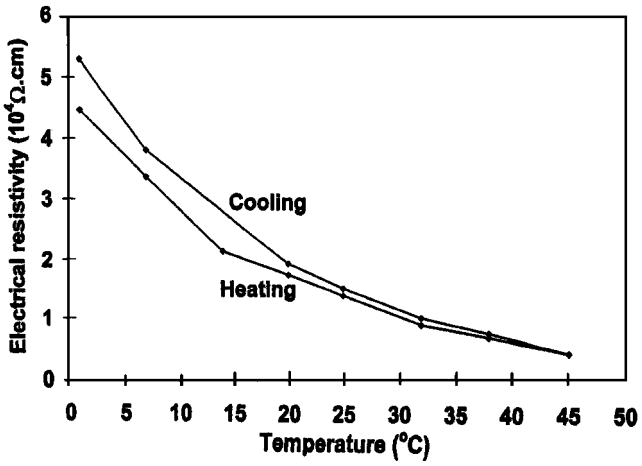

Fig. 3 Plot of fume electrical resistivity vs temperature during heating and cooling for carbon-fiber silica-fume cement paste

Table 1 Resistivity, Critical Voltage, and Activation Energy of Five Types of Cement Paste

Formulation	Resistivity at 20°C (Ω.m)	Critical Voltage at 20°C (V)	Activation Energy (eV)	
			Heating	Cooling
Plain	$(4.87 \pm 0.37) \times 10^3$	10.80 ± 0.45	0.040 ± 0.006	0.122 ± 0.006
Silica fume	$(6.12 \pm 0.15) \times 10^3$	11.60 ± 0.37	0.035 ± 0.003	0.084 ± 0.004
Carbon fibers + silica fume	$(1.73 \pm 0.08) \times 10^2$	8.15 ± 0.34	0.390 ± 0.014	0.412 ± 0.017
Latex	$(6.99 \pm 0.12) \times 10^3$	11.80 ± 0.31	0.017 ± 0.001	0.025 ± 0.002
Carbon fibers + latex	$(9.64 \pm 0.08) \times 10^2$	8.76 ± 0.35	0.018 ± 0.001	0.027 ± 0.002

teristic starts to deviate from linearity is referred to as the critical voltage.

Figure 3 shows a plot of the resistivity vs temperature during heating and cooling for carbon-fiber silica-fume cement paste. The resistivity decreases upon heating and the effect is quite reversible upon cooling. That the resistivity is slightly increased after a heating-cooling cycle is probably due to thermal degradation of the material.

Figure 4 shows the Arrhenius plot of log conductivity (conductivity = 1/resistivity) vs reciprocal absolute temperature. The slope of the plot gives the activation energy, which is 0.390 ± 0.014 and 0.412 ± 0.017 eV during heating and cooling, respectively. This energy corresponds to the barrier for electron motion across the interface between carbon fiber and cement paste.[1] The contact resistivity of this interface is around 50 $\Omega.m^2$, as obtained by single-fiber electromechanical pullout testing.[46] The contact resistivity is dependent on the fiber surface treatment and is higher when latex is present in the cement paste.[46]

Results similar to those of carbon-fiber silica-fume cement paste were obtained with carbon-fiber (0.5% by weight of cement) latex (20% by weight of cement) cement paste, silica-fume cement paste, latex cement paste, and plain cement paste. However, for all four types of cement paste, (i) the resistivity is higher by about an order of magnitude, and (ii) the activation energy is lower by about an order of magnitude, as shown in Table 1. The critical voltage is higher when fibers are absent (Table 1).

It is of practical significance that the sensitivity of a carbon-fiber silica-fume cement paste as a thermistor, as indicated by the activation energy given above, is comparable to that of semiconductor thermistors. For mortar without conducting fibers, the activation energy of conduction has been reported to be only 2×10^{-4} eV,[53] as indicated by impedance measurement. More study is needed for mortars.

4. Effect of Strain on Resistive Behavior

Piezoresistivity (to be distinguished from piezoelectricity) is a phenomenon in which the electrical resistivity of a material changes with strain, which relates to stress. This phenomenon allows a material to serve as a strain/stress sensor. Applications of the stress/strain sensors include pressure sensors for aircraft and automobile components, vibration sensors for civil structures such as bridges, and weighing-in-motion sensors for highways (weighing of vehicles). The first category tends to involve small sensors (e.g., in the form of cement paste or mortar) and they will compete with silicon pressure sensors. The second and third categories tend to involve large sensors (e.g., in the form of precast concrete or mortar) and they will compete with silicon, acoustic, inductive, and pneumatic sensors.

Piezoresistivity studies have been mostly conducted on polymer-matrix composites with fillers that are electrically conducting. These composite piezoresistive sensors work because strain changes the proximity between the conducting filler units, thus affecting the electrical resistivity. Tension in-

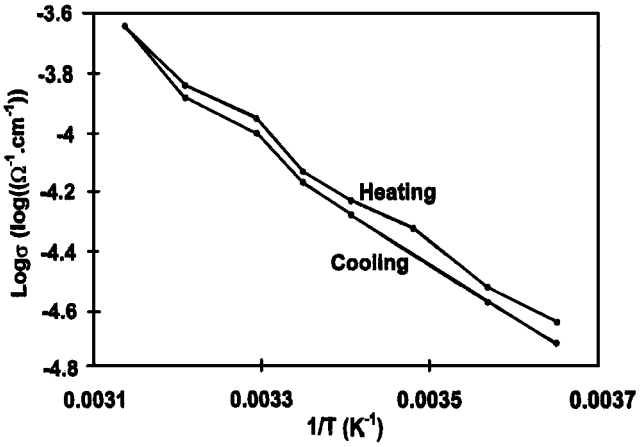

Fig. 4 Arrhenius plot of log electrical conductivity vs reciprocal absolute temperature for carbon-fiber silica-fume cement paste

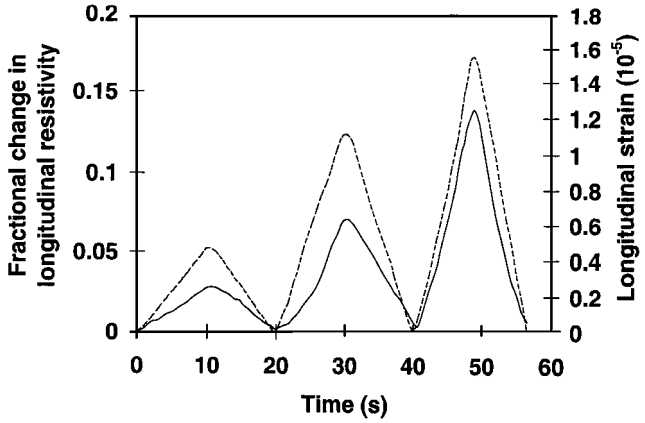

Fig. 5 Variation of the fractional change in longitudinal electrical resistivity with time (solid curve) and of the strain with time (dashed curve) during dynamic uniaxial tensile loading at increasing stress amplitudes within the elastic regime for carbon-fiber silica-fume cement paste

creases the distance between the filler units, thus increasing the resistivity; compression decreases this distance, thus decreasing the resistivity.

Piezoresistivity in a structural material, such as a continuous fiber polymer-matrix composite, is particularly attractive, because the structural material becomes an intrinsically smart material that senses its own strain without the need for embedded or attached strain sensors. Not needing embedded or attached sensors means lower cost, greater durability, larger sensing volume (with the whole structure being able to sense), and the absence of mechanical property degradation (which occurs in the case of embedded sensors).

The electrical resistance of a carbon-fiber cement-matrix composite changes reversibly with strain such that the gage factor (fractional change in resistance per unit strain) is up to 700 under compression or tension.[54-68] Both resistance (DC) and reactance (AC) increase reversibly upon tension and decreases reversibly upon compression because of fiber pullout upon microcrack openings (<1 μm) and the consequent increase in fiber-matrix contact resistivity. The concrete contains as low as 0.2 vol.% short carbon fibers, which are preferable to those that have been surface treated. The fibers do not need to touch one another in the composite. The treatment improves the wetability with water. The presence of a large aggregate decreases the gage factor, but the strain sensing ability remains sufficient for practical use. Strain sensing concrete works even when data acquisition is wireless. The applications include structural vibration control and traffic monitoring.

Figures 5 and 6 show the fractional changes in the longitudinal and transverse resistivities, respectively, for carbon-fiber silica-fume cement paste at 28 days of curing during repeated uniaxial tensile loading at increasing strain amplitudes.[62] The strain essentially returns to zero at the end of each cycle, indicating elastic deformation. The longitudinal strain is positive (i.e., elongation); the transverse strain is negative (i.e., shrinkage due to the Poisson effect). Both longitudinal and transverse resistivities increase reversibly upon uniaxial tension. The reversibility of both strain and resistivity is more complete in the longitudinal direction than the transverse direction. The gage factor is 89 and −59 for the longitudinal and transverse resistances, respectively.

Figures 7 and 8[64] show corresponding results for silica-fume cement paste (without fiber). The strain is essentially entirely reversible in both the longitudinal and transverse directions, but the resistivity is only partly reversible in both directions, in contrast to the reversibility of the resistivity when fibers are present (Fig. 5 and 6). As is the case with fibers, both longitudinal and transverse resistivities increase upon uniaxial tension. However, the gage factor is only 7.2 and −7.1 for Fig. 7 and 8, respectively. Comparison of Fig. 5 and 6 (with fibers) with Fig. 7 and 8 (without fibers) shows that fibers greatly enhance the magnitude and reversibility of the resistivity effect. The gage factors are much smaller in magnitude when fibers are absent.

The increase in both longitudinal and transverse resistivities upon uniaxial tension for cement pastes, whether with or without fibers, is attributed to defect generation.[64] In the presence of fibers, fiber bridging across microcracks occurs and slight fiber pullout occurs upon tension, thus enhancing the possibility of microcrack closing and causing more reversibility in the resistivity change. The fibers are much more electrically conductive than the cement matrix. The presence of the fibers introduces interfaces between fibers and matrix. The degradation of the fiber-matrix interface due to fiber pullout or other mechanisms is an additional type of defect generation, which will increase the resistivity of the composite. Therefore, the presence of fibers greatly increases the gage factor.

The transverse resistivity increases upon uniaxial tension even though the Poisson effect causes the transverse strain to be negative. This means that the effect of the transverse resistivity increase overshadows the effect of the transverse shrinkage. The resistivity increase is a consequence of the uniaxial tension. In contrast, under uniaxial compression, the resistance in the stress direction decreases at 28 days of curing. Hence, the effects of uniaxial tension on the transverse resistivity and of uniaxial compression on the longitudinal resistivity are different; the gage factors are negative and positive for these cases, respectively.

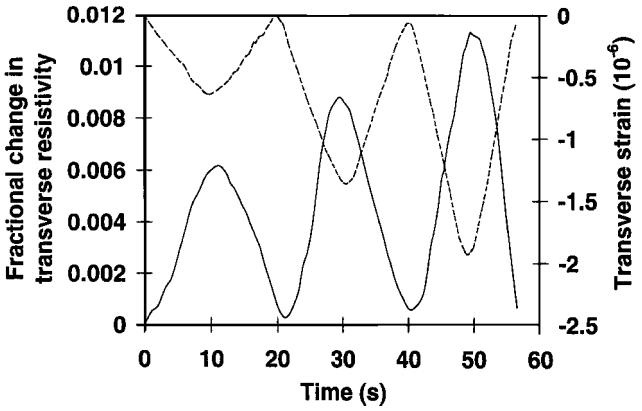

Fig. 6 Variation of the fractional change in transverse electrical resistivity with time (solid curve) and of the strain with time (dashed curve) during dynamic uniaxial tensile loading at increasing stress amplitudes within the elastic regime for carbon-fiber silica-fume cement paste

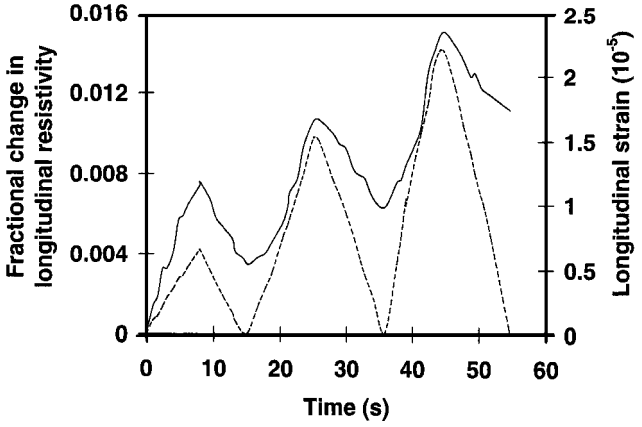

Fig. 7 Variation of the fractional change in longitudinal electrical resistivity with time (solid curve) and of the strain with time (dashed curve) during dynamic uniaxial tensile loading at increasing stress amplitudes within the elastic regime for silica-fume cement paste

The similarity of the resistivity change in longitudinal and transverse directions under uniaxial tension suggests similarity for other directions as well. This means that the resistance can be measured in any direction to sense the occurrence of tensile loading. Although the gage factor is comparable in both longitudinal and transverse directions, the fractional change in resistance under uniaxial tension is much higher in the longitudinal direction than the transverse direction. Thus, the use of the longitudinal resistance for practical self-sensing is preferred.

Piezoresistivity also occurs in cement-matrix composites with continuous carbon fibers.[69] The electrical resistance in the fiber direction, as measured using surface electrical contacts, increases upon tension in the same direction. The resistance increase is mostly reversible such that the irreversible portion increases with the stress amplitude. The effect is attributed to fiber-matrix interface degradation, which is partly irreversible. The gage factor is up to 60.

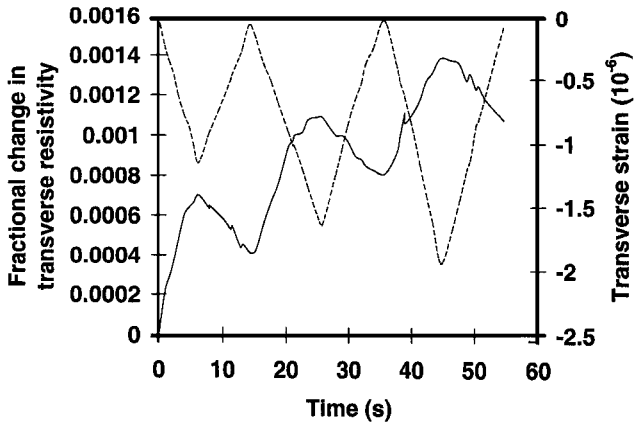

Fig. 8 Variation of the fractional change in transverse electrical resistivity with time (solid curve) and of the strain with time (dashed curve) during dynamic uniaxial tensile loading at increasing stress amplitudes within the elastic regime for silica-fume cement paste

5. Effect of Damage on Resistive Behavior

Concrete, whether with or without admixtures, is capable of sensing major and minor damage—even damage during elastic deformation—as a result of the electrical resistivity increase that accompanies damage.[55,59,64,70] That both strain and damage can be sensed simultaneously through resistance measurement means that the strain/stress condition (during dynamic loading) under which damage occurs can be obtained, thus facilitating damage origin identification. Damage is indicated by a resistance increase, which is larger and less reversible when the stress amplitude is higher. The resistance increase can be a sudden increase during loading. It can also be a gradual shift of the baseline resistance.

Figure 9(a)[64] shows the fractional change in resistivity along the stress axis as well as the strain during repeated compressive loading at an increasing stress amplitude for plain cement paste at 28 days of curing. Figure 9(b) shows the corresponding variation of stress and strain during the repeated loading. The strain varies linearly with the stress up to the highest stress amplitude (Fig. 9b). The strain returns to zero at the end of each cycle of loading. During the first loading, the resistivity increases due to damage initiation. During the subsequent unloading, the resistivity continues to increase, probably as a result of the opening of the microcracks generated during loading. During the second loading, the resistivity decreases slightly as the stress increases up to the maximum stress of the first cycle (probably due to closing of the microcracks) and then increases as the stress increases beyond this value (probably due to the generation of additional microcracks). During unloading in the second cycle, the resistivity increases significantly (probably due to opening of the microcracks). During the third loading, the resistivity essentially does not change (or decreases very slightly) as the stress increases to the maximum stress of the third cycle (probably due to the balance between microcrack generation and microcrack closing). Subsequent unloading causes the resistivity to increase very significantly (probably due to opening of the microcracks).

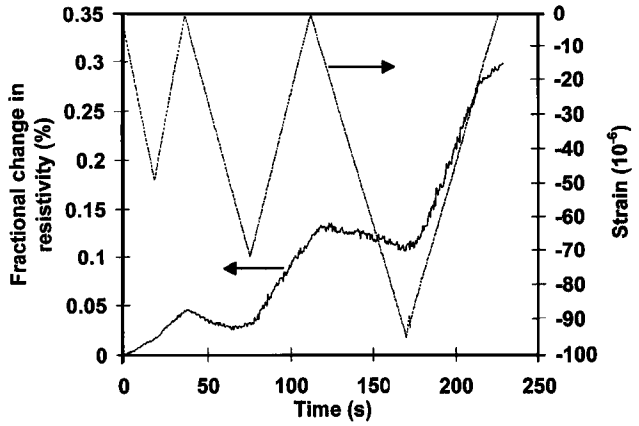

(a)

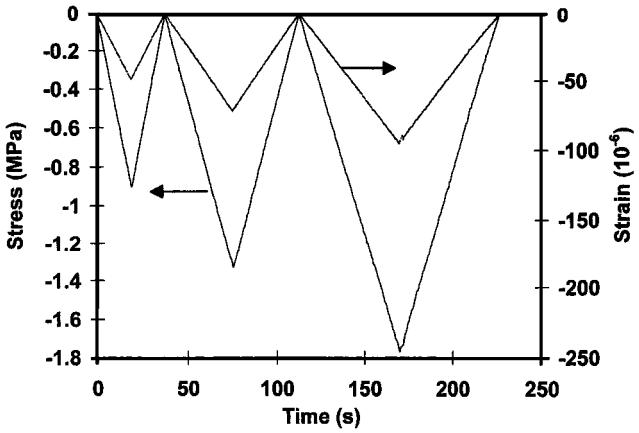

(b)

Fig. 9 Variation of the fractional change in electrical resistivity with time **(a),** of the stress with time **(b),** and of the strain (negative for compressive strain) with time (a and b) during dynamic compressive loading at increasing stress amplitudes, within the elastic regime for silica-fume cement paste at 28 days of curing

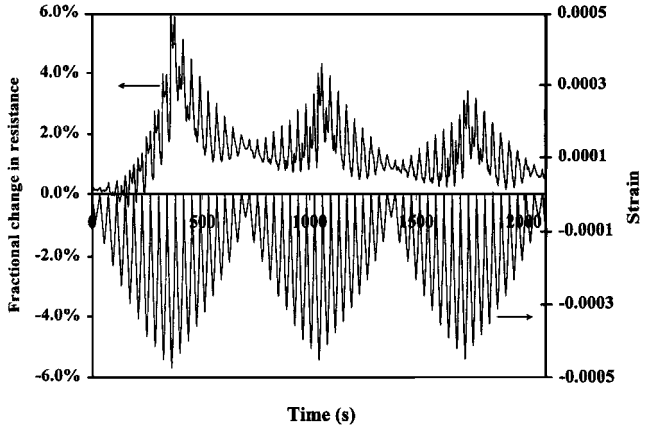

(a)

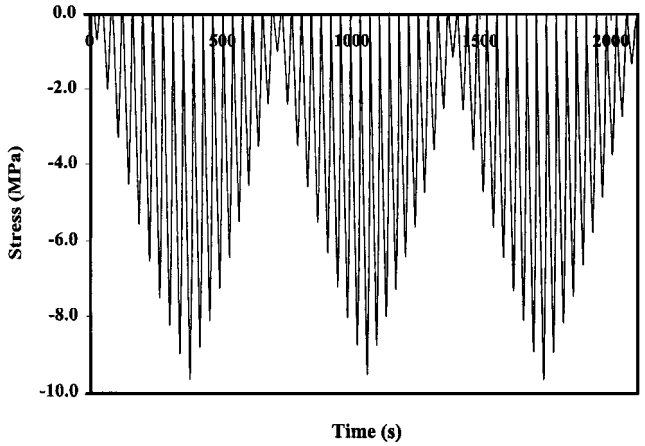

(b)

Fig. 10 Fractional change in resistance **(a),** strain (a), and stress **(b)** during repeated compressive loading at increasing and decreasing stress amplitudes, the highest of which was 60% of the compressive strength, for carbon fiber concrete at 28 days of curing

Figure 10[70] shows the fractional change in resistance, strain and stress during repeated compressive loading at increasing and decreasing stress amplitudes for carbon fiber (0.18 vol.%) concrete (with fine and coarse aggregates) at 28 days of curing. The highest stress amplitude is 60% of the compressive strength. A group of cycles in which the stress amplitude increases cycle by cycle and then decreases cycle by cycle back to the initial low stress amplitude is hereby referred to as a group. Figure 10[70] shows the results for three groups. The strain returns to zero at the end of each cycle for any of the stress amplitudes, indicating elastic behavior. The resistance decreases upon loading in each cycle, as in Fig. 4. An extra peak at the maximum stress of a cycle grows as the stress amplitude increases, resulting in two peaks per cycle. The original peak (strain induced) occurs at zero stress, whereas the extra peak (damage induced) occurs at the maximum stress. Hence, during loading from zero stress within a cycle, the resistance drops and then increases sharply, reaching the maximum resistance of the extra peak at the maximum stress of the cycle. Upon subsequent unloading, the resistance decreases and then increases as unloading continues, reaching the maximum resistance of the original peak at zero stress. In the part of this group where the stress amplitude decreases cycle by cycle, the extra peak diminishes and disappears, leaving the original peak as the sole peak. In the part of the second group where the stress amplitude increases cycle by cycle, the original peak (peak at zero stress) is the sole peak, except that the extra peak (peak at the maximum stress) returns in a minor way (more minor than in the first group) as the stress amplitude increases. The extra peak grows as the stress amplitude increases, but, in the part of the second group in which the stress amplitude decreases cycle by cycle, it quickly diminishes and vanishes, as in the first group. Within each group, the amplitude of resistance variation increases as the stress amplitude increases and decreases as the stress amplitude subsequently decreases.

The greater the stress amplitude, the larger and the less reversible is the damage-induced resistance increase (the extra peak). If the stress amplitude has been experienced before, the damage-induced resistance increase (the extra peak) is small, as shown by comparing the result of the second group with that of the first group (Fig. 10), unless the extent of damage is large (Fig. 11[70] for the highest stress amplitude of >90% the com-

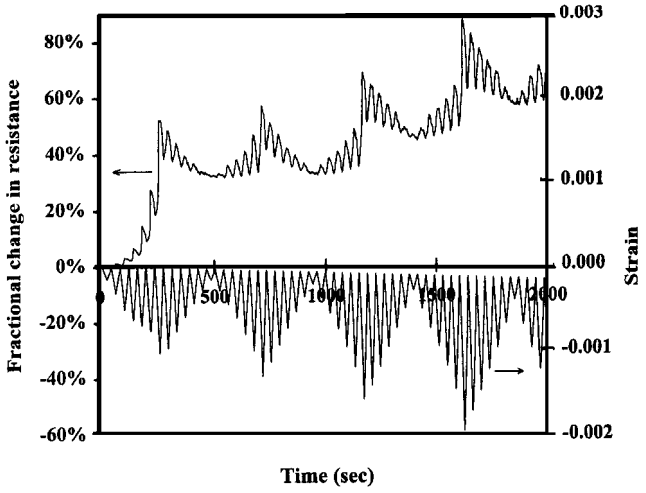

(a)

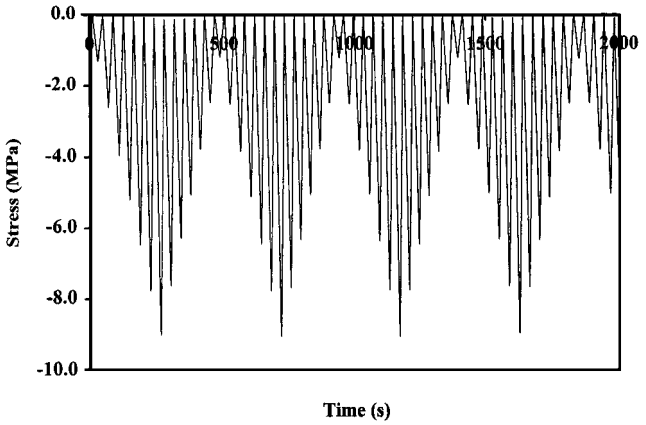

(b)

Fig. 11 Fractional change in resistance **(a),** strain (a), and stress **(b)** during repeated compressive loading at increasing and decreasing stress amplitudes, the highest of which was >90% of the compressive strength, for carbon fiber concrete at 28 days of curing

pressive strength). When the damage is extensive (as shown by a modulus decrease), a damage-induced resistance increase occurs in every cycle, even at a decreasing stress amplitude, overshadowing the strain-induced resistance decrease (Fig. 11). Hence, the damage-induced resistance increase occurs mainly during loading (even within the elastic regime), particularly at a stress above that in previous cycles, unless the stress amplitude is high and/or damage is extensive.

At a high-stress amplitude, the damage-induced resistance increases cycle by cycle as the stress amplitude increases causes the baseline resistance to increase irreversibly (Fig. 11). The baseline resistance in the regime of major damage (with a decrease in modulus) provides a measure of the extent of damage (i.e., condition monitoring). This measure works in the loaded or unloaded state. In contrast, the measure using the damage-induced resistance increase (Fig. 10) works only during stress increase and indicates the occurrence of damage (whether minor or major) as well as the extent of damage.

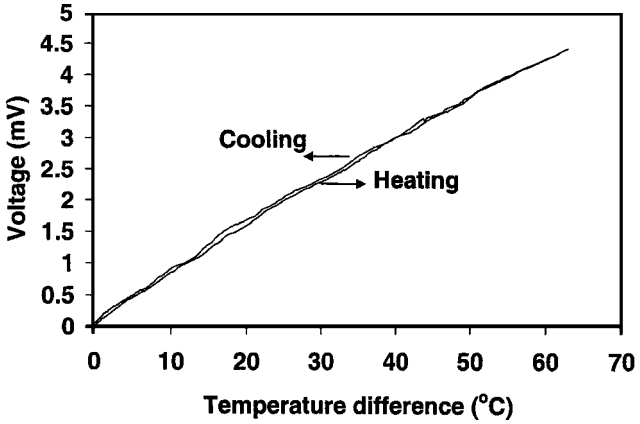

Fig. 12 Variation of the Seebeck voltage (with copper as the reference) vs the temperature difference during heating and cooling for steel-fiber silica-fume cement paste containing steel fibers in the amount of 1.0% by weight of cement

6. Thermoelectric Behavior

The Seebeck effect[2,44,71-73] is a thermoelectric effect (i.e., an effect involving the conversion between thermal energy and electrical energy) which is the basis for thermocouples for temperature measurement. It also allows the conversion from thermal energy to electrical energy. This effect involves charge carriers moving from a hot point to a cold point within a material, thereby resulting in a voltage difference between the two points. The Seebeck coefficient is the voltage difference (hot minus cold) per unit temperature difference (hot minus cold) between the two points. Negative carriers (electrons) make it more negative and positive carriers (holes) make it more positive.

The Seebeck effect in carbon fiber reinforced cement paste involves electrons from the cement matrix[2] and holes from the fibers[71-73] such that the two contributions are equal at the percolation threshold, with a fiber content between 0.5% and 1.0% by weight of cement.[2] The hole contribution increases monotonically with increasing fiber content below and above the percolation threshold.[2] It also increases with intercalation of the carbon fibers with an acceptor such as bromine,[18] so that absolute thermoelectric power reaches +17 μV/°C (Table 2).

As a result of the free electrons in a metal, cement containing metal fibers such as steel fibers is even more negative (as negative as −69 μV/°C, Table 2) in the thermoelectric power than cement without fiber.[44] The attainment of a very positive thermoelectric power is attractive because a material with a positive thermoelectric power and a material with negative thermoelectric power are two very dissimilar materials, the junction of which is a thermocouple junction. (The greater the dissimilarity, the more sensitive is the thermocouple.) A cement-based thermocouple and electric current rectification have been attained by using a cement-based pn-junction.[74]

Thermopower results are shown in Table 2 and Fig. 12. The absolute thermoelectric power is much more positive for all the steel-fiber cement pastes compared to all the carbon-fiber cement pastes. An increase of the steel fiber content from 0.5%

Table 2 Volume Electrical Resistivity and Absolute Thermoelectric Power of Various Cement Pastes with Steel Fibers (S_f), Pristine Carbon Fibers (C_f), or Intercalated Carbon Fibers (C_f')

Cement Paste	Volume Fraction Fibers	Resistivity (Ω.m)	Absolute Thermoelectric Power (μV/°C)
Plain	0	$(4.7 \pm 0.4) \times 10^3$	−1.99 ± 0.03
SF	0	$(5.8 \pm 0.4) \times 10^3$	−2.03 ± 0.02
L	0	$(6.8 \pm 0.6) \times 10^3$	−2.06 ± 0.02
S_f (0.5) (*)	0.10%	$(7.8 \pm 0.5) \times 10^2$	−53.3 ± 4.8
S_f (1.0) (*)	0.20%	$(4.8 \pm 0.4) \times 10^2$	−59.1 ± 5.2
S_f (0.5) + SF (*)	0.10%	$(5.6 \pm 0.5) \times 10^2$	−57.1 ± 3.9
S_f (1.0) + SF (*)	0.20%	$(3.2 \pm 0.3) \times 10^2$	−68.5 ± 4.5
S_f (0.5) + L (*)	0.085%	$(1.4 \pm 0.1) \times 10^3$	−50.4 ± 3.2
S_f (1.0) + L (*)	0.17%	$(1.1 \pm 0.1) \times 10^3$	−57.7 ± 5.0
C_f (0.5) + SF (*)	0.48%	$(1.5 \pm 0.1) \times 10^2$	−0.89 ± 0.09
C_f (1.0) + SF (*)	0.95%	8.3 ± 0.5	+0.48 ± 0.11
C_f (0.5) + L (*)	0.41%	$(9.7 \pm 0.6) \times 10^2$	−1.14 ± 0.05
C_f (1.0) + L (*)	0.82%	$(1.8 \pm 0.2) \times 10^1$	−0.24 ± 0.08
C_f' (0.5*) + SF	0.4%	/	+11.5 ± 1.13
C_f' (1.0*) + SF	0.8%	/	+16.6 ± 1.32
C_f' (0.5*) + L	0.3%	/	+7.42 ± 1.09
C_f' (1.0*) + L	0.7%	/	+10.2 ± 1.07

(*) % by weight of cement
SF: silica fume; L: latex

to 1.0% by weight of cement increases the absolute thermoelectric power, whether silica fume (or latex) is present or not. An increase of the steel fiber content also increases the reversibility and linearity of the change in Seebeck voltage with the temperature difference between the hot and cold ends, as shown by comparing the values of the Seebeck coefficient obtained during heating and cooling in Table 2. The values obtained during heating and cooling are close for the pastes with the higher steel fiber content but not so close for the pastes with the lower steel fiber content. In contrast, for pastes with carbon fibers in place of steel fibers, the change in Seebeck voltage with the temperature difference is highly reversible for both carbon fiber contents of 0.5% and 1.0% by weight of cement, as shown in Table 2 by comparing the values of the Seebeck coefficient obtained during heating and cooling.

Table 2 shows that the volume electrical resistivity is much higher for the steel-fiber cement pastes than the corresponding carbon fiber cement pastes. This is attributed to the much lower volume fraction of fibers in the former (Table 2). An increase in the steel or carbon fiber content from 0.5% to 1.0% by weight of cement decreases the resistivity, although this decrease is more significant in the case of the carbon fiber than the steel fiber. That the resistivity decrease is not large when the steel fiber content is increased from 0.5% to 1.0% by weight of cement and that the resistivity is still high at a steel fiber content of 1.0% by weight of cement suggest that a steel fiber content of 1.0% by weight of cement is below the percolation threshold.

Whether with or without silica fume (or latex), the change of the Seebeck voltage with temperature is more reversible and linear at a steel fiber content of 1.0% by weight of cement than at a steel fiber content of 0.5% by weight of cement. This is attributed to the larger role of the cement matrix at the lower steel fiber content and the contribution of the cement matrix to the irreversibility and non-linearity. Irreversibility and non-linearity are particularly significant when the cement paste contains no fiber.

From the practical point of view, the steel-fiber silica-fume cement paste containing steel fibers in the amount of 1.0% by weight of cement is particularly attractive for use in temperature sensing, as the absolute thermoelectric power is the highest (−68 μV/°C) and the variation of the Seebeck voltage with the temperature difference between the hot and cold ends is reversible and linear. The absolute thermoelectric power is as high as those of commercial thermocouple materials.

7. Electromagnetic Behavior

Cement-matrix composites interact with electromagnetic radiation by reflection and absorption. The reflection component can be greatly enhanced by the use of an electrically conductive admixture, such as short carbon fibers.

EMI shielding refers to the reflection and/or adsorption of electromagnetic radiation by a material, which thereby acts as a shield against the penetration of the radiation through the shield. As electromagnetic radiation, particularly that at high frequencies (e.g., radio waves, such as those emanating from cellular phones) tend to interfere with electronics (e.g., computers), EMI shielding of both electronics and radiation source is needed and is increasingly required by governments around the world. The importance of EMI shielding relates to the high demand of today's society on the reliability of electronics and the rapid growth of radio frequency radiation sources.

Electromagnetic radiation at high frequencies penetrates only the near surface region of an electrical conductor. This is known as the skin effect. Due to the skin effect, a composite material having a conductive filler with a small unit size (e.g., particle size, fiber diameter, etc.) of the filler is more effective than one having a conductive filler with a large unit size of the

filler. For effective use of the entire cross-section of a filler unit for shielding, the unit size of the filler should be comparable to or less than the skin depth. Therefore, a filler of unit size 1 μm or less is typically preferred, though such a small unit size is not commonly available for most fillers and the dispersion of the filler is more difficult when the filler unit size decreases.

Cement is slightly conducting; therefore, the use of a cement matrix also allows the conductive filler units in the composite to be electrically connected, even when the filler units do not touch one another. Thus, cement-matrix composites have higher shielding effectiveness than corresponding polymer-matrix composites in which the polymer matrix is insulating.[75] A shielding effectiveness of 40 dB at 1 GHz has been attained in a cement-matrix composite containing just 1.5 vol.% discontinuous 0.1 μm-diameter carbon filaments.[76] Moreover, cement is less expensive than polymers and cement-matrix composites are useful for the shielding of rooms in a building.[76-78] In addition, the reflectivity renders the ability to provide lateral guidance in the automatic highway technology, as a traffic lane with a radio wave reflecting concrete as an overlay in either the middle portion or the edge portions along the length of the lane reflects the wave emitted from a vehicle that is installed with a radio wave transmitter and receiver.[75]

A disadvantage of EMI shielding is the inability of penetration of television signals. The combined use of carbon fibers and beads alleviates this problem.[79]

The interaction of electromagnetic radiation with concrete can also be utilized for nondestructive evaluation.[80,81] For this application, high reflectivity is not desirable.

8. Conclusion

The resistive, piezoresistive, thermoelectric, and electromagnetic behavior of cement-matrix composites can be greatly modified by the use of admixtures, such as short carbon fibers and short steel fibers. Short carbon fibers are effective in enhancing the piezoresistive behavior and enhancing the effect of damage on the resistive behavior. Short carbon fibers are effective in enhancing the p-type Seebeck effect, whereas short steel fibers are effective for enhancing the n-type Seebeck effect. Submicron diameter carbon filaments are effective for enhancing the electromagnetic reflection behavior.

Acknowledgment

This work was supported in part by National Science Foundation.

References

1. S. Wen and D.D.L. Chung: "Carbon Fiber-Reinforced Cement as a Thermistor," *Cem. Concr. Res.,* 1999, *29*(6), pp. 961-65.
2. S. Wen and D.D.L. Chung: "Seebeck Effect in Carbon Fiber Reinforced Cement," *Cem. Concr. Res.,* 1999, *29*(12), pp. 1989-93.
3. X. Fu and D.D.L. Chung: "Degree of Dispersion of Latex Particles in Cement Paste, as Assessed by Electrical Resistivity Measurement," *Cem. Concr. Res.,* 1996, *26*(7), pp. 985-91.
4. P.J. Tumidajski: "Electrical Conductivity of Portland Cement Mortars," *Cem. Concr. Res.,* 1996, *26*(4), pp. 529-34.
5. G. Ping, X. Ping, and J.J. Beaudoin: "Microstructural Characterization of the Transition Zone in Cement Systems by Means of A.C. Impedance Spectroscopy," *Cem. Concr. Res.,* 1993, *23*(3), pp. 581-91.
6. T.O. Mason, S.J. Ford, J.D. Shane, J.-H. Hwang, and D.D. Edwards: "Experimental Limitations in Impedance Spectroscopy of Cement-Based Materials," *Adv. Cem. Res.,* 1998, *10*(4), pp. 143-50.
7. D.E. MacPhee, D.C. Sinclair, and S.L. Stubbs: "Electrical Characterization of Pore Reduced Cement by Impedance Spectroscopy," *J. Mater. Sci. Letters,* 1996, *15*(18), pp. 1566-68.
8. S.L. Cormack, D.E. MacPhee, and D.C. Sinclair: "AC Impedance Spectroscopy Study of Hydrated Cement Pastes," *Adv. Cem. Res.,* 1998, *10*(4), pp. 151-59.
9. M. Keddam, H. Takenouti, X.R. Novoa, C. Andrade, and C. Alonso: "Impedance Measurements on Cement Paste," *Cem. Concr. Res.,* 1997, *27*(8), pp. 1191-201.
10. W.J. McCarter and G. Starrs: "Impedance Characterization of Ordinary Portland Cement-Pulverized Fly Ash Binders," *J. Mater. Sci. Lett.,* 1997, *16*(8), pp. 605-07.
11. P. Gu and J.J. Beaudoin: "Dielectric Behaviour of Hardened Cement Paste Systems," *J. Mater Sci. Letters,* 1996, *15*(2), pp. 182-84.
12. Z. Xu, P. Gu, P. Xie, and J.J. Beaudoin: "Application of A.C. Impedance Techniques in Studies of Porous Cementitious Materials," *Cem. Concr. Res.,* 1993, *23*(4), 1993, pp. 853-62.
13. S.J. Ford, T.O. Mason, B.J. Christensen, R.T. Coverdale, H.M. Jennings, and E.J. Garboczi, Electrode Configurations and Impedance Spectra of Cement Pastes, *J. Mater. Sci.,* 1995, *30*(5), pp. 1217-24.
14. P. Gu, Z. Xu, P. Xie, and J.J. Beaudoin: "Application of A.C. Impedance Techniques in Studies of Porous Cementitious Materials. (I): Influence of Solid Phase and Pore Solution on High Frequency Resistance," *Cem. Concr. Res.,* 1993, *23*(3), pp. 531-40.
15. P.-W. Chen, X. Fu, and D.D.L. Chung: "Microstructural and Mechanical Effects of Latex, Methylcellulose and Silica Fume on Carbon Fiber Reinforced Cement," *ACI Mater. J.,* 1997, *94*(2), pp. 147-55.
16. P. Chen and D.D.L. Chung: "Improving the Electrical Conductivity of Composites Comprised of Short Conducting Fibers in a Non-Conducting Matrix: the Addition of a Non-Conducting Particulate Filler," *J. Electron. Mater.,* 1995, *24*(1), pp. 47-51.
17. Z. Shui, J. Li, F. Huang, and D. Yang: "Study on the Electrical Properties of Carbon Fiber-Cement Composite (CFCC)," *J. Wuhan Univ. Tech.,* 1995, *10*(4), pp. 37-41.
18. S. Wen, and D.D.L. Chung. "Effect of Carbon Fiber Grade on the Electrical Behavior of Carbon Fiber Reinforced Cement," *Carbon,* 2001, *39*, pp 369-73.
19. S. Wen, and D.D.L. Chung: "Electric Polarization in Carbon Fiber Reinforced Cement," *Cem. Concr. Res.,* 2001, *31*(2), pp. 141-47.
20. X. Fu and D.D.L. Chung: "Carbon Fiber Reinforced Mortar as an Electrical Contact Material for Cathodic Protection," *Cem. Concr. Res.*, 1995, *25*(4), pp. 689-94.
21. M.S. Morsy: "Effect of Temperature on Electrical Conductivity of Blended Cement Pastes," *Cem. Concr. Res.,* 1999, *29*, pp. 603-06.
22. J.G. Wilson and N.K. Gupta: "Assessment of Structure Formation in Fresh Concrete by Measurement of its Electrical Resistance," *Building Res. Info.,* 1996, *24*(4), pp. 209-12.
23. S.A. Abo El-Enein, M.F. Kotkata, G.B. Hanna, M. Saad, and M.M. Abd El Razek: "Electrical Conductivity of Concrete Containing Silica Fume," *Cem. Concr. Res.,* 1995, *25*(8), pp. 1615-20.
24. H.C. Kim, S.Y. Kim, and S.S. Yoon: "Electrical Properties of Cement Paste Obtained from Impedance Spectroscopy," *J. Mater. Sci.,* 1995, *30*(15), pp. 3768-772.
25. C. Alonso, C. Andrade, M. Keddam, X.R. Novoa, and H. Takenouti: "Study of the Dielectric Characteristics of Cement Paste," *Mater. Sci. Forum,* pt 1, 1998, *289-292*, pp. 15-28.
26. P. Gu, P. Xie, J.J. Beaudoin, and R. Brousseau: "A.C. Impedance Spectroscopy (II): Microstructural Characterization of Hydrating Cement-Silica Fume Systems," *Cem. Concr. Res.,* 1993, *23(*1), pp. 157-68.
27. P. Xie, P. Gu, Z. Xu, and J.J. Beaudoin: "Rationalized A.C. Impedance Model for Microstructural Characterization of Hydrating Cement Systems," *Cem. Concr. Res.,* 1993, *23*(2), pp. 359-67.
28. P. Gu, P. Xie, Y. Fu, and J.J. Beaudoin: "A.C. Impedance Phenomena in Hydrating Cement Systems: Frequency Dispersion Angle and Pore Size Distribution," *Cem. Concr. Res.,* 1994, *24*(1), pp. 86-88.
29. P. Gu, P. Xie, Y. Fu, and J.J. Beaudoin: "A.C. Impedance Phenomena

in Hydrating Cement Systems: the Drying-Rewetting Process," *Cem. Concr. Res.,* 1994, *24*(1), pp. 89-91.
30. P. Xie, P. Gu, Y. Fu, and J.J. Beaudoin: "A.C. Impedance Phenomena in Hydrating Cement Systems: Detectability of the High Frequency Arc," *Cem. Concr. Res.,* 1994, *24*(1), pp. 92-94.
31. P. Xie, P. Gu, Y. Fu, and J.J. Beaudoin: "A.C. Impedance Phenomena in Hydrating Cement Systems: Origin of the High Frequency Arc," *Cem. Concr. Res.,* 1994, *24*(4), pp. 704-6.
32. P. Gu, P. Xie, and J.J. Beaudoin: "Determination of Silica-Fume Content in Hardened Concrete by AC Impedance Spectroscopy," *Cem. Concr. Aggregates,* 1995, *17*(1), pp. 92-97.
33. W.J. McCarter: "Parametric Study of the Impedance Characteristics of Cement-Aggregate Systems During Early Hydration," *Cem. Concr. Res.,* 1994, *24*(6), pp. 1097-110.
34. B.J. Christensen, R.T. Coverdale, R.A. Olson, S.J. Ford, E.J. Garboczi, H.M. Jennings, and T.O. Mason: "Impedance Spectroscopy of Hydrating Cement-Based Materials: Measurement, Interpretation, and Application," *J. Am. Ceramic Soc.,* 1994, *77*(11), pp. 2789-804.
35. P. Gu, P. Xie, and J.J. Beaudoin: "Some Applications of AC Impedance Spectroscopy in Cement Research," *Cem. Concr. Aggregates,* 1995, *17*(2), pp. 113-18.
36. P. Xie, P. Gu, and J.J. Beaudoin: "Contact Capacitance Effect in Measurement of A.C. Impedance Spectra for Hydrating Cement Systems," *J. Mater. Sci.,*1996, *31*(1), pp. 144-49.
37. S.S. Yoon, H.C. Kim, and R.M. Hill: "Dielectric Response of Hydrating Porous Cement Paste," *J. Physics D-Appl. Physics,* 1996, *29*(3), pp. 869-75.
38. G.M. Moss, D.J. Christensen, T.O. Mason, and H.M. Jennings: "Microstructural Analysis of Young Cement Pastes Using Impedance Spectroscopy During Pore Solution Exchange," *Adv. Cem. Based Mater.,*1996, *4*(2), pp. 68-75.
39. W.J. McCarter: "A.C. Impedance Response of Concrete During Early Hydration," *J. Mater. Sci.,* 1996, *31*(23), pp. 6285-92.
40. S.J. Ford, J.-H. Hwang, J.D. Shane, R.A. Olson, G.M. Moss, H.M. Jennings, and T.O. Mason: "Dielectric Amplification in Cement Pastes," *Adv. Cem. Based Mater.,* 1997, *5*(2), pp. 41-48.
41. J.M. Torrents and R. Pallas-Areny: "Measurement of Cement Setting by Impedance Monitoring," in *Conf. Record—IEEE Instrumentation and Measurement Technology Conference, 2,* 1997, IEEE, Piscataway, NJ, pp. 1089-93.
42. J.M. Torrents, J. Roncero, and R. Gettu: "Utilization of Impedance Spectroscopy for Studying the Retarding Effect of a Superplasticizer on the Setting of Cement," *Cem. Concr. Res.,* 1998, *28*(9), pp. 1325-33.
43. C. Andrade, V.M. Blanco, A. Collazo, M. Keddam, X.R. Nova, and H. Takenouti, "Cement Paste Hardening Process Studied by Impedance Spectroscopy," *Electrochimica Acta.,* 1999, *44*(24), pp. 4313-18.
44. S. Wen, and D.D.L. Chung: "Seebeck Effect in Steel Fiber Reinforced Cement," *Cem. Concr. Res.,* 2000, *30*(4), pp. 661-64.
45. X. Fu, and D.D.L. Chung: "Single Fiber Electromechanical Pull-Out Testing and Its Application to Studying the Interface Between Steel Fiber and Cement," *Composite Interfaces,* 1997, *4*(4), pp. 197-211.
46. X. Fu, W. Lu, and D.D.L. Chung: "Improving the Bond Strength between Carbon Fiber and Cement by Fiber Surface Treatment and Polymer Addition to Cement Mix," *Cem. Concr. Res.,*1996, *26*(7), pp. 1007-12.
47. X. Fu, and D.D.L. Chung: "Interface Between Steel Rebar and Concrete Studied by Electromechanical Pull-Out Testing," *Composite Interfaces,* 1999, *6*(2), pp. 81-92.
48. D.E. Wilkosz, and J.F. Young: "Effect of Moisture Adsorption on the Electrical Properties of Hardened Portland Cement Compacts," *J. Am. Ceram. Soc.,* 1995, *78*(6), pp. 1673-79.
49. D. Buerchler, B. Elsener, and H. Boehni: "Electrical Resistivity and Dielectric Properties of Hardened Cement Paste and Mortar," *Mat. Res. Soc. Symp. Proc.* 1996, *411*, pp. 407-12.
50. M. Saleem, M. Shameem, S.E. Hussain, and M. Maslehuddin: "Effect of Moisture, Chloride and Sulphate Contamination on the Electrical Resistivity of Portland Cement Concrete," *Construction & Building Mater.,* 1996, *10*(3), pp. 209-14.
51. B.P. Borglum, J.F. Young, and R.C. Buchanan: "Electrical Properties of Chemically Bonded Ceramics Based on Calcium Aluminate," *Adv. Cem. Bas. Mat.,* 1993, *1*(1), pp. 47-50.
52. J.F. Young: "Cement-Based Chemically Bonded Electrical Ceramics," *Mat. Tech.,* 1994, *9*(3/4), pp. 63-67.
53. W.J. McCarter: "Effects of Temperature on Conduction and Polarization in Portland Cement Mortar," *J. Am. Ceramic Soc.,* 1995, *78*(2), pp. 411-15.
54. X. Fu, W. Lu, and D.D.L. Chung: "Ozone Treatment of Carbon Fiber for Reinforcing Cement," *Carbon,* 1998, *36*(9), pp. 1337-45.
55. P. Chen and D.D.L. Chung: "Carbon Fiber Reinforced Concrete as a Smart Material Capable of Non-Destructive Flaw Detection," *Smart Mater. Struct.,* 1993, *2,* pp. 22-30.
56. P. Chen and D.D.L. Chung: "Concrete as a New Strain/Stress Sensor," *Composites*, Part B, 1996, *27*B, pp. 11-23.
57. P. Chen, and D.D.L. Chung: "Carbon Fiber Reinforced Concrete as an Intrinsically Smart Concrete for Damage Assessment During Dynamic Loading," *J. Am. Ceram. Soc.,* 1995, *78*(3), pp. 816-18.
58. D.D.L. Chung: "Strain Sensors Based on the Electrical Resistance Change Accompanying the Reversible Pull-Out of Conducting Short Fibers in a Less Conducting Matrix," *Smart Mater. Struct.,* 1995, *4*, pp. 59-61.
59. P. Chen, and D.D.L. Chung: "Carbon Fiber Reinforced Concrete as an Intrinsically Smart Concrete for Damage Assessment During Static and Dynamic Loading," *ACI Mater. J.,* 1996, *93(*4), pp. 341-50.
60. X. Fu, and D.D.L. Chung, "Self-Monitoring of Fatigue Damage in Carbon Fiber Reinforced Cement," *Cem. Concr. Res.,* 1996, *26*(1), pp. 15-20.
61. X. Fu, E. Ma, D.D.L. Chung, and W.A. Anderson: "Self-Monitoring in Carbon Fiber Reinforced Mortar by Reactance Measurement," *Cem. Concr. Res.* 1997, *27*(6), pp. 845-52.
62. X. Fu and D.D.L. Chung: "Effect of Curing Age on the Self-Monitoring Behavior of Carbon Fiber Reinforced Mortar," *Cem. Concr. Res.* 1997, *27*(9), pp. 1313-18.
63. X. Fu, W. Lu, and D.D.L. Chung: "Improving the Strain Sensing Ability of Carbon Fiber Reinforced Cement by Ozone Treatment of the Fibers," *Cem. Concr. Res.* 1998, *28*(2), pp. 183-87.
64. D.D.L. Chung: "Carbon Fiber Cement-Matrix Composites," *TANSO,* 1999, *190*, pp. 300-12.
65. Z. Shi, and D.D.L. Chung: "Carbon Fiber Reinforced Concrete for Traffic Monitoring and Weighing in Motion," *Cem. Concr. Res.,* 1999, *29*(3), pp. 435-39.
66. Q. Mao, B. Zhao, D. Sheng, and Z. Li: "Resistance Changement of Compression Sensible Cement Speciment Under Different Stresses," *J. Wuhan Univ. Tech., Mater. Sci. Ed.,* 1996, *11*(3), pp. 41-45.
67. Q. Mao, B. Zhao, D. Shen, and Z. Li: "Study on the Compression Sensibility of Cement Matrix Carbon Fiber Composite," *Fuhe Cailiao Xuebao/Acta Materiae Compositae Sinica,* 1996, *13*(4), pp. 8-11.
68. M. Sun, Q. Mao, and Z. Li: "Size Effect and Loading Rate Dependence of the Pressure-Sensitivity of Carbon Fiber Reinforced Concrete (CFRC)," *J. Wuhan Univ. Tech.*, Mater. Sci. Ed., 1998, *13*(4), pp. 58-61.
69. S. Wen and D.D.L. Chung: "Piezoresistivity in Continuous Carbon Fiber Cement-Matrix Composite," *Cem. Concr. Res.,* 1999, *29*(3), pp. 445-49.
70. D. Bontea, D.D.L. Chung, and G.C. Lee: "Damage in Carbon Fiber Reinforced Concrete, Monitored by Electrical Resistance Measurement," *Cem. Concr. Res.,* 2000, *30*(4), pp. 651-59.
71. M. Sun, Z. Li, Q. Mao, and D. Shen: "A Study on Thermal Self-Monitoring of Carbon Fiber Reinforced Concrete," *Cem. Concr. Res.,* 1999, *29*(5), pp. 769-71.
72. M. Sun, Z. Li, Q. Mao, and D. Shen: "Thermoelectric Percolation Phenomena in Carbon Fiber-Reinforced Concrete," *Cem. Concr. Res.,* 1998, *28*(12), pp. 1707-12.
73. M. Sun, Z. Li, Q. Mao, and D. Shen: "Study on the Hole Conduction Phenomenon in Carbon Fiber-Reinforced Concrete," *Cem. Concr. Res.,* 1998, *28*(4), pp. 549-54.
74. S. Wen, and D.D.L. Chung: "Rectifying and Thermocouple Junctions Based on Portland Cement," *J. Mater. Res.,* 2001, *16*(7), pp. 1989-93.
75. X. Fu and D.D.L. Chung: "Submicron-Diameter-Carbon-Filament Cement-Matrix Composites," *Carbon,* 1998, *36*(4), pp. 459-62.
76. L. Gnecco: "Building a Shielded Room is Not Construction 101," *Evaluation Eng.,* 1999, *38*(3), p. 3.

77. S.-S. Lin: "Application of Short Carbon Fiber in Construction," *SAMPE J.* 1994, *30*(5), pp. 39-45.
78. Y. Kurosaki and R. Satake: "Relationshipp. Between the Effectiveness of Electromagnetic Shielded Rooms and the Effectiveness of Shielding Materials," *IEEE Int. Symp. Electromagnetic Compatibility*. IEEE, Piscataway, NJ, 1994, pp. 739-40.
79. Y. Shimizu, A. Nishikata, N. Maruyama, and A. Sugiyama: "Absorbing Concrete for TV-Frequency Mixed With Carbon Fibers and Beads," *Nippon Terebijon Gakkaishi (J. Inst. Television Eng. Jpn.),* 1986, *40*(8), pp. 780-85.
80. I.L. Al-Qadi, O.A. Hazim, W. Su, and S.M. Riad: "Dielectric Properties of Portland Cement Concrete at Low Radio Frequencies," *J. Mater. Civil Eng.,* 1995, 7(3), pp. 192-98.
81. O. Buyukozturk, and H.C. Rhim: "Modeling of Electromagnetic Wave Scattering by Concrete Specimens," *Cem. Concr. Res.,* 1995, *25*(5), pp. 1011-22.